

MSM71 - LOBSTER: Basin opening and inversion insights from seismic data in the Ligurian Sea

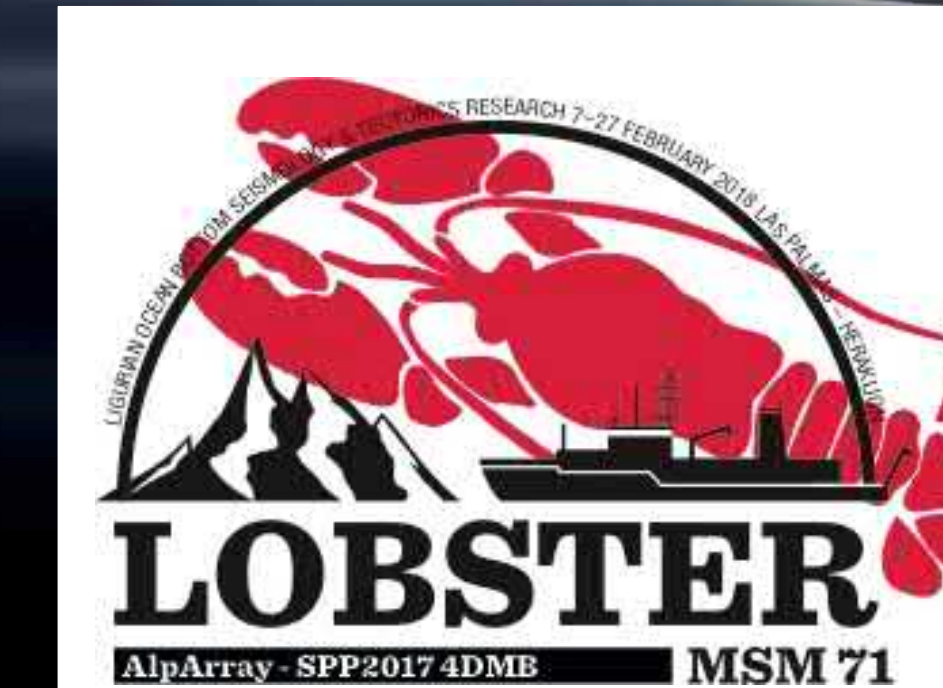
Anke Dannowski¹, Martin Thorwart², Ingo Grevemeyer¹, Heidrun Kopp^{1,2}, Grazia Caielli³, Roberto de Franco³, Dietrich Lange¹, W.C. Crawford⁴, A. Paul⁵, MSM71 cruise participants, and the AlpArray Working Group

Contact: adannowski@geomar.de

¹ GEOMAR, Helmholtz Zentrum für Ozeanforschung, Kiel, Germany
² CAU, Christian-Albrechts-Universität zu Kiel, Germany
³ IDPA-CNR, Istituto per la dinamica dei processi ambientali, Sezione di Milano, Italy

⁴ IGP, Laboratoire de Géosciences Marines, Institut de Physique du Globe de Paris, France
⁵ ISTERRE, Univ. Grenoble Alpes Univ. Savoie Mont Blanc, CNRS, IRD, UGE, Grenoble, France

Statuskonferenz
 Forschungsschiffe
 22./23.02.2022

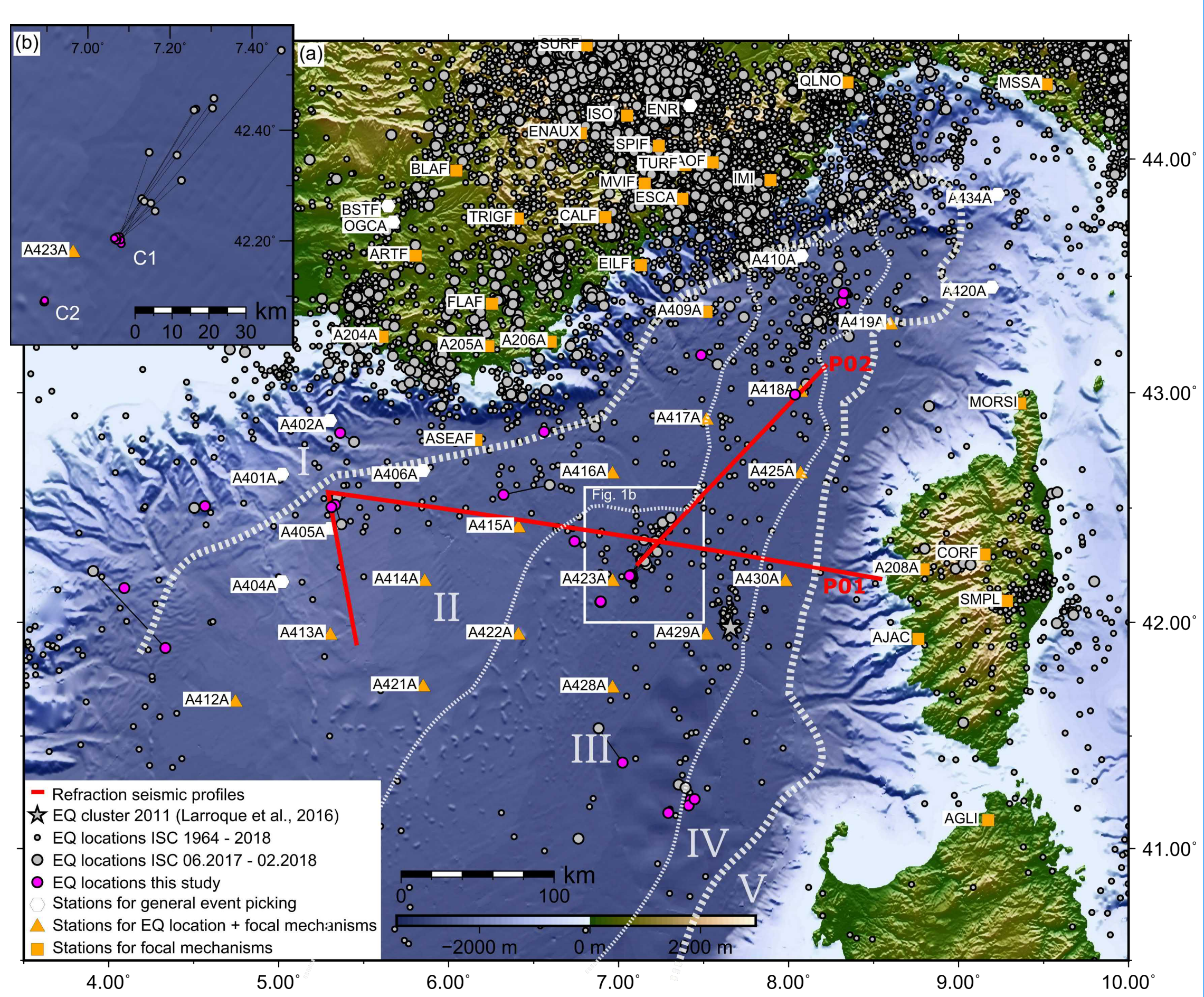


Introduction

The Liguro-Provençal Basin, located in the Mediterranean Sea, was generated by the south-eastward trench retreat of the Apennines-Calabrian subduction zone, from Late Oligocene to Miocene. The extension led to extreme continental thinning. Today, local seismicity indicates a closure of the basin.

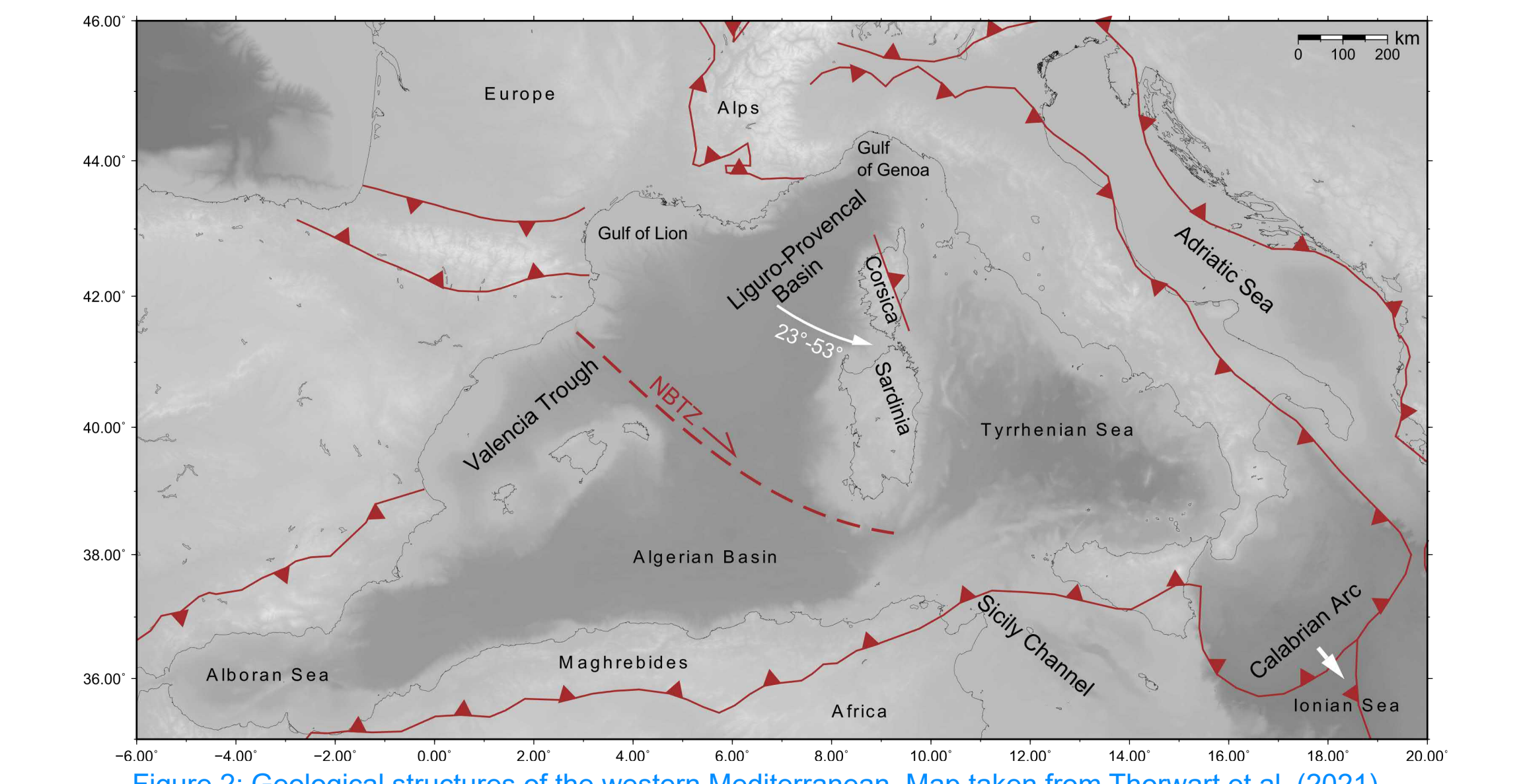
To shed light on the present day lithospheric architecture of the Ligurian Basin, we acquired state of the art seismic data during MSM71 onboard RV Maria S. Merian. Ocean bottom seismometers (OBS) were recovered that recorded for 8 months local to global seismicity in the framework of SPP2017 4D-MB, the German component of the European AlpArray initiative.

Figure 1: (a) New seismic refraction transects (red lines) cross the Ligurian Basin. White dotted lines mark proposed limits of the continental (I, V), transitional (II, IV) and oceanic domains with an atypical oceanic crust (III) (Gueguen et al., 1998; Rollet et al., 2002). Orange triangles and squares show locations of the long-term OBS and land stations used in our analysis. (b) Location of two seismic clusters observed in our study.



Geological background

- ~30 Ma: Rifting initiated associated with magmatism on land along the Ligurian coast
- ~21 Ma: Rifting terminated; anti-clockwise rotation of the Corsica-Sardinia block initiated → opening of the Ligurian Sea
- ~16 Ma: Opening of the Ligurian Basin terminated; a second calc-alkaline volcanic phase along the Corsican margin
- ~8 Ma: Extension shifted east of Corsica opening of the Tyrrhenian Sea until



Data

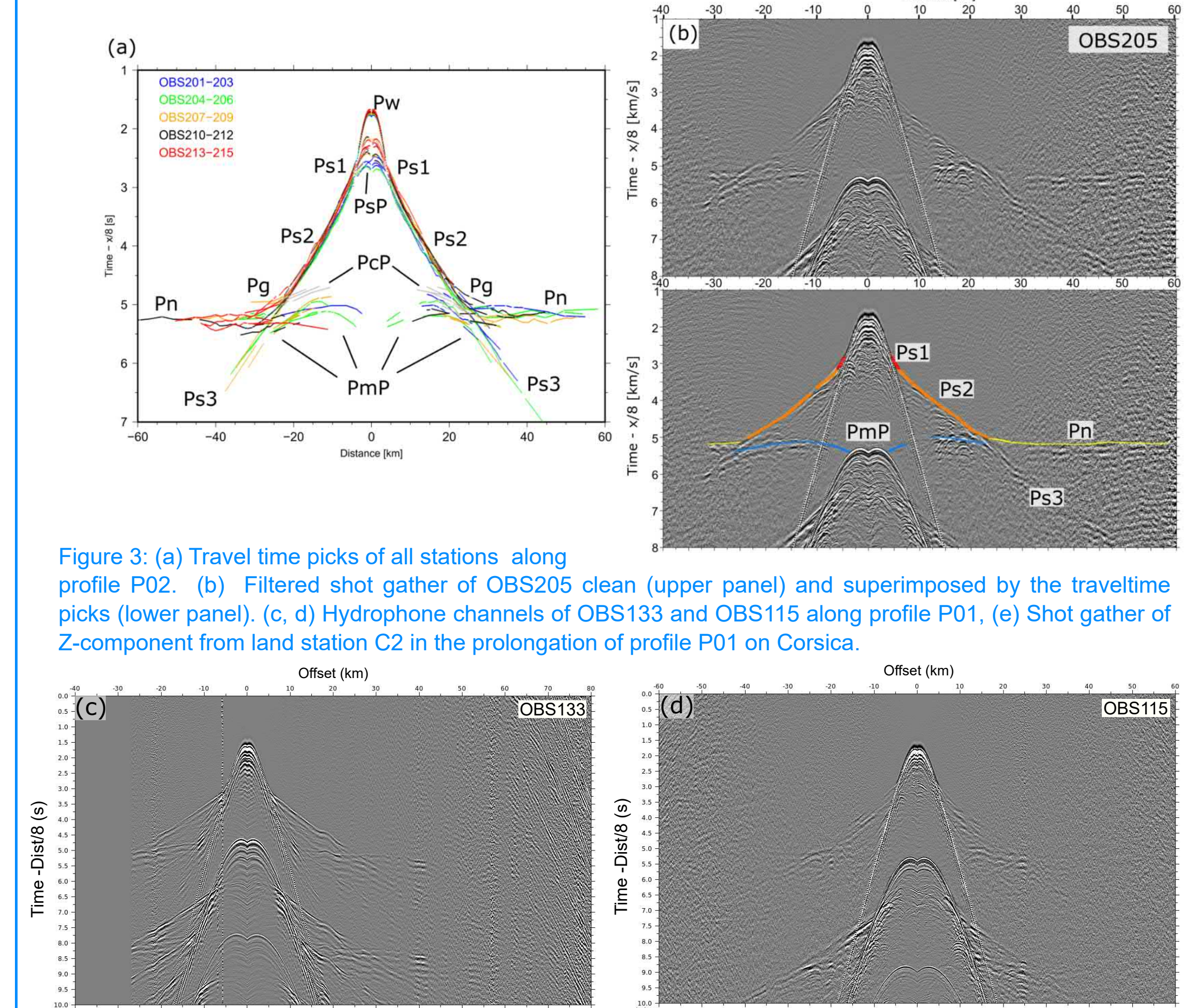


Figure 3: (a) Travel time picks of all stations along profile P02. (b) Filtered shot gather of OBS205 clean (upper panel) and superimposed by the traveltime picks (lower panel). (c, d) Hydrophone channels of OBS133 and OBS115 along profile P01. (e) Shot gather of Z-component from land station C2 in the prolongation of profile P01 on Corsica.

Data acquired during MSM71 onboard RV Maria S. Merian:

- Active seismic shots recorded on ocean bottom seismometer (OBS) and on land stations
- Multi-channel seismic and Parasound data
- Stations from the AlpArray OBS network were recovered that recorded the local and global seismicity.

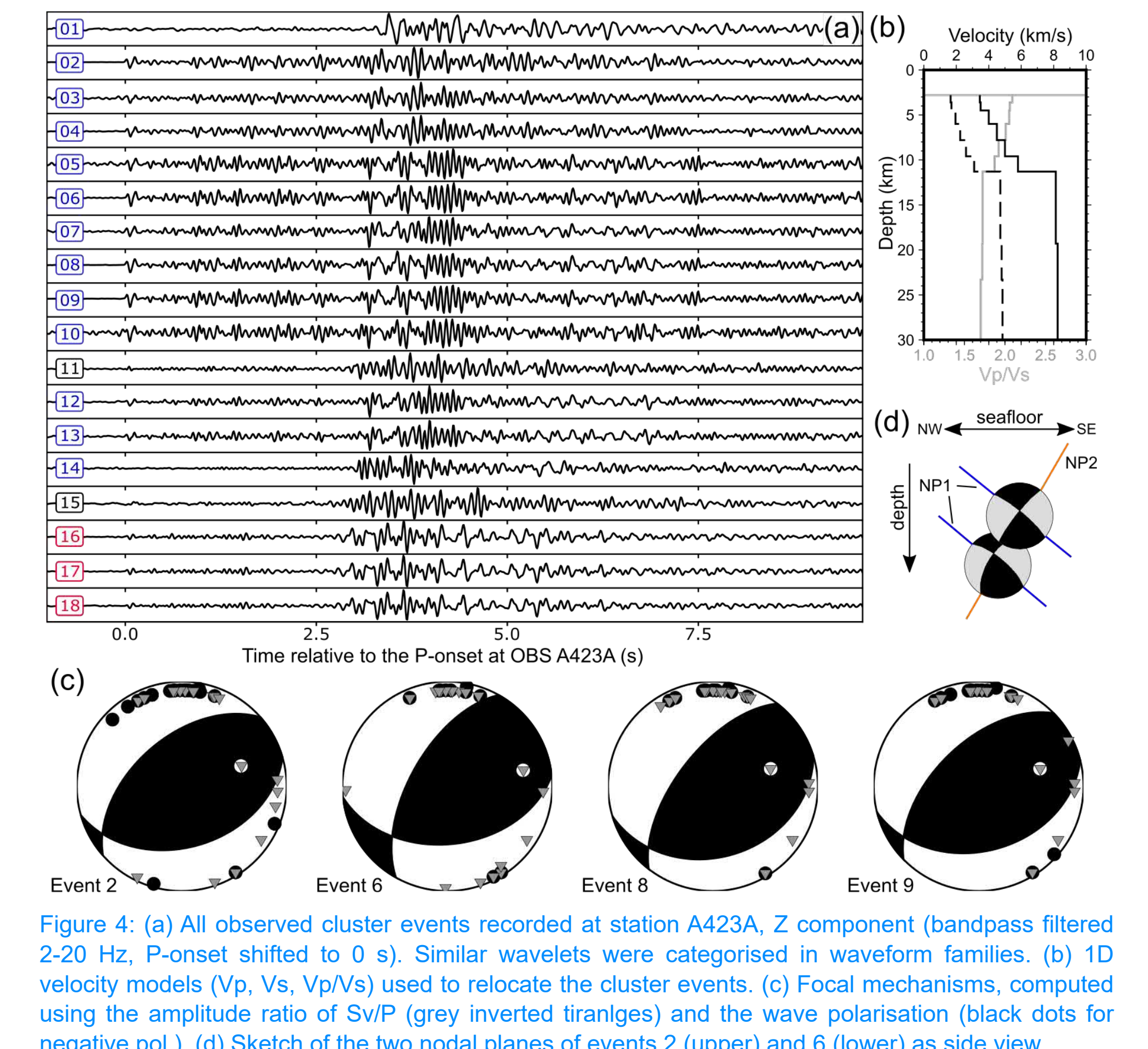


Figure 4: (a) All observed cluster events recorded at station A423A. Z component (bandpass filtered 2-20 Hz, P-onset shifted to 0 s). Similar wavelets were categorised in waveform families. (b) 1D velocity models (Vp, Vs, Vp/Vs) used to relocate the cluster events. (c) Focal mechanisms, computed using the amplitude ratio of Sv/P (grey inverted triangles) and the wave polarisation (black dots for negative pol.). (d) Sketch of the two nodal planes of events 2 (upper) and 6 (lower) as side view.

Results

Travel time tomography

- Plio-Quaternary sediments, Messinian salt, Pre-Messinian to syn-rift sediments from the seafloor down to the acoustic basement
- Strong velocity contrast (6.6 km/s to >7.5 km/s) at the seismic Moho
- Absence of seismic velocities between 6.6 km/s and 7.3 km/s in the basin → no fresh oceanic crust material, possibly continental crust

Gravity modeling

- Seismic velocity to density conversion after Christensen and Mooney (1995) and Carlson and Miller (2003) to fit observed satellite gravity.

Local seismicity

- 39 events in the basin centre
- Two clusters (C1, 13 events and C2, 3 events)
- Vp/Vs=1.72 and Vs=4.7 km/s
- Epicentres in the uppermost mantle

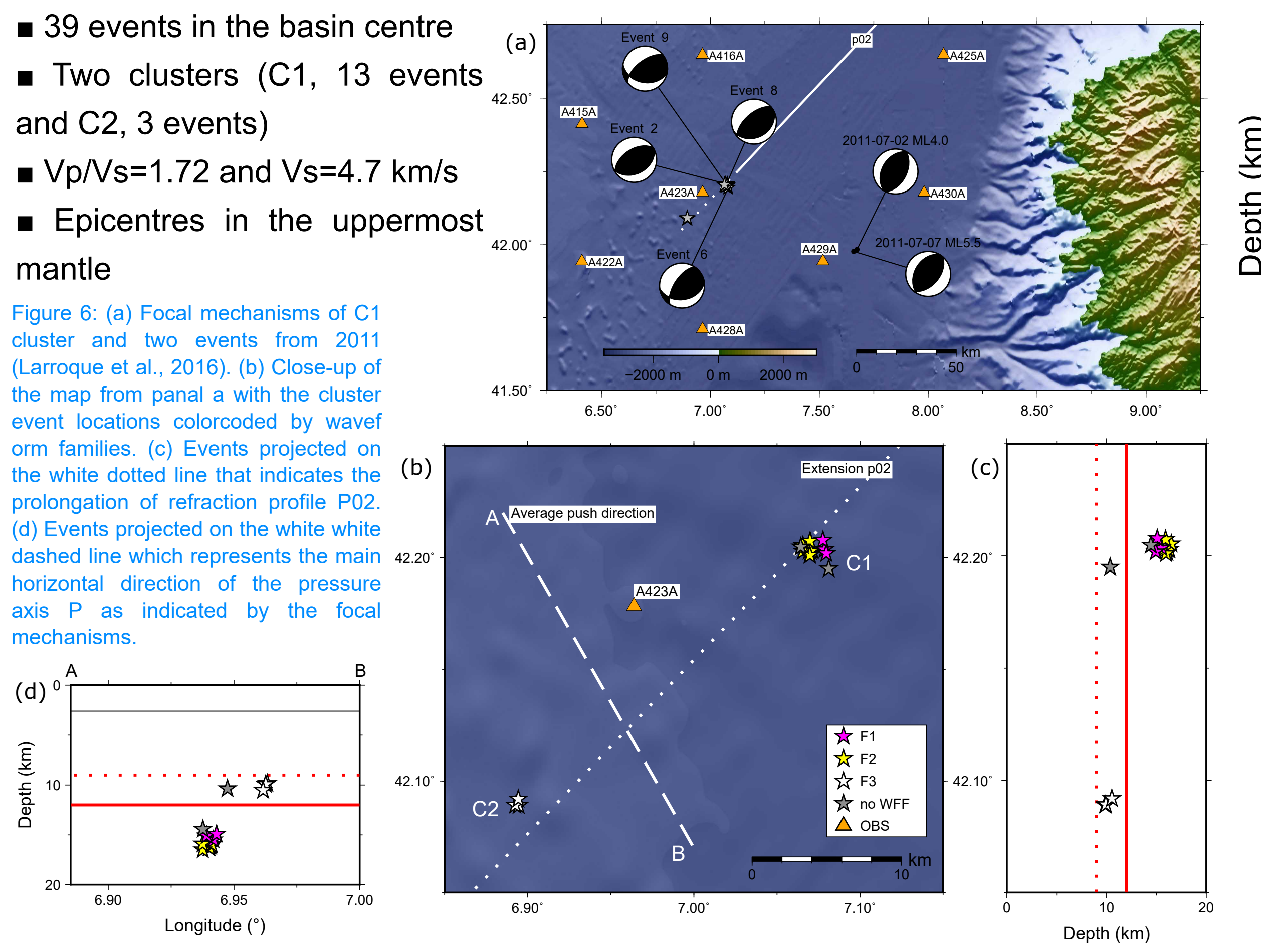


Figure 6: (a) Focal mechanisms of C1 cluster and two events from 2011 (Larroque et al., 2016). (b) Close-up of the map from panel a with the cluster event locations color-coded by waveform families. (c) Events projected on the white dotted line that indicates the prolongation of refraction profile P02. (d) Events projected on the white dashed line which represents the main horizontal direction of the pressure axis P as indicated by the focal mechanisms.

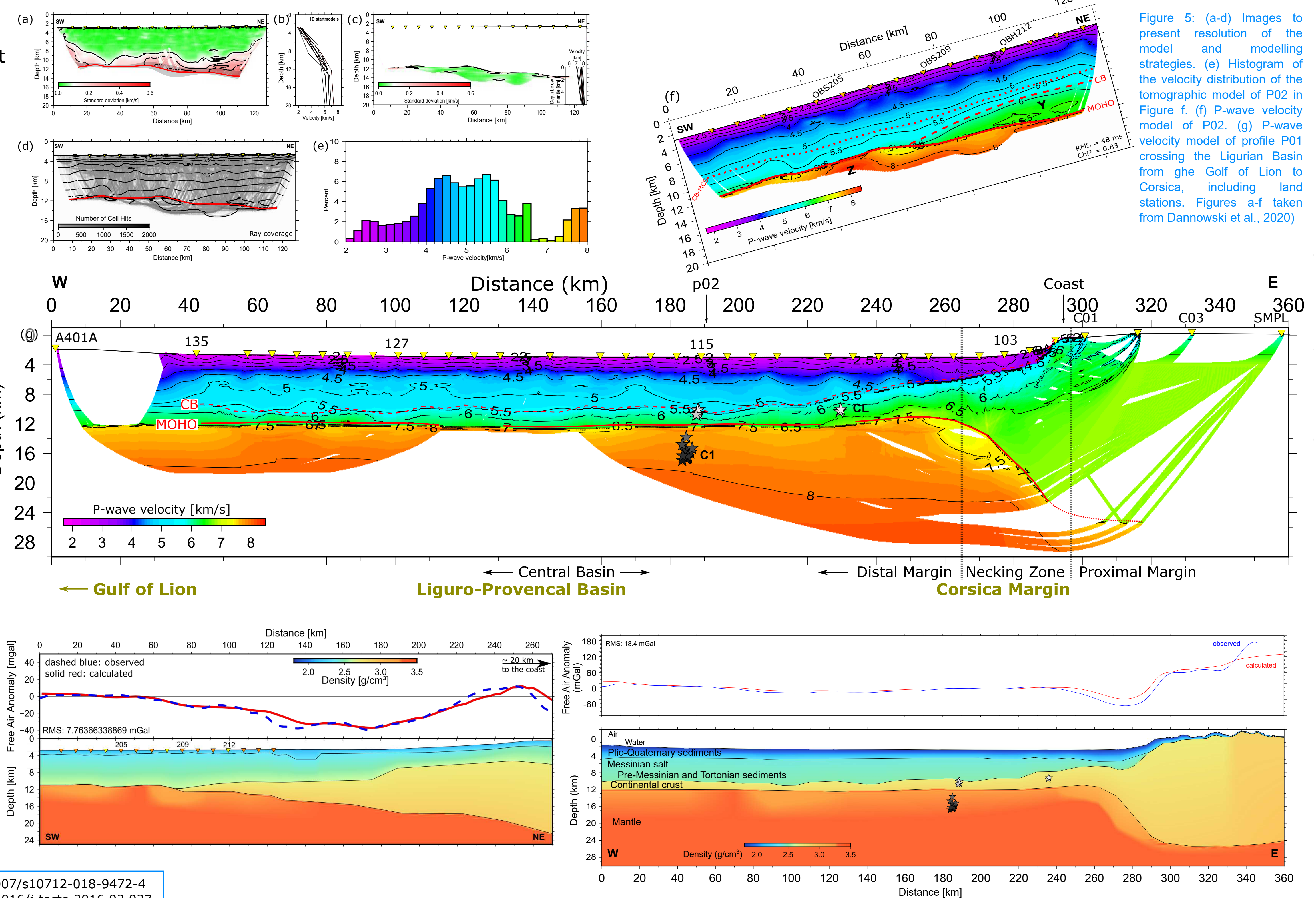


Figure 7: Results from forward gravity modelling for P02 (left figure) and P01 (right figure). The lower panels show the density models derived from the seismic velocity models and minor adjustments to the densities. Upper panels present the data fit between the observed free-air anomaly data (blue line) and the model response (red line).

Discussion

Nature of the lithosphere

Typical oceanic crust consists of Layer 2 with a high-velocity gradient and Layer 3 with a low-velocity gradient. Typical seismic velocities of Layer 3 are ~6.5 km/s < Vp < 7.2 km/s. We observe seismic velocities ~5.5 km/s < Vp < 6.6 km/s, interpreted as continental crust. Between 110 km and 160 km, along profile P01, Pn phases are strongly attenuated.

- No indication for oceanic crust or oceanic spreading in the velocity profiles
- Seismic energy attenuated due to Messinian salt or serpentinised mantle?
- Wider necking zone at the Gulf of Lion compared to the Corsica margin

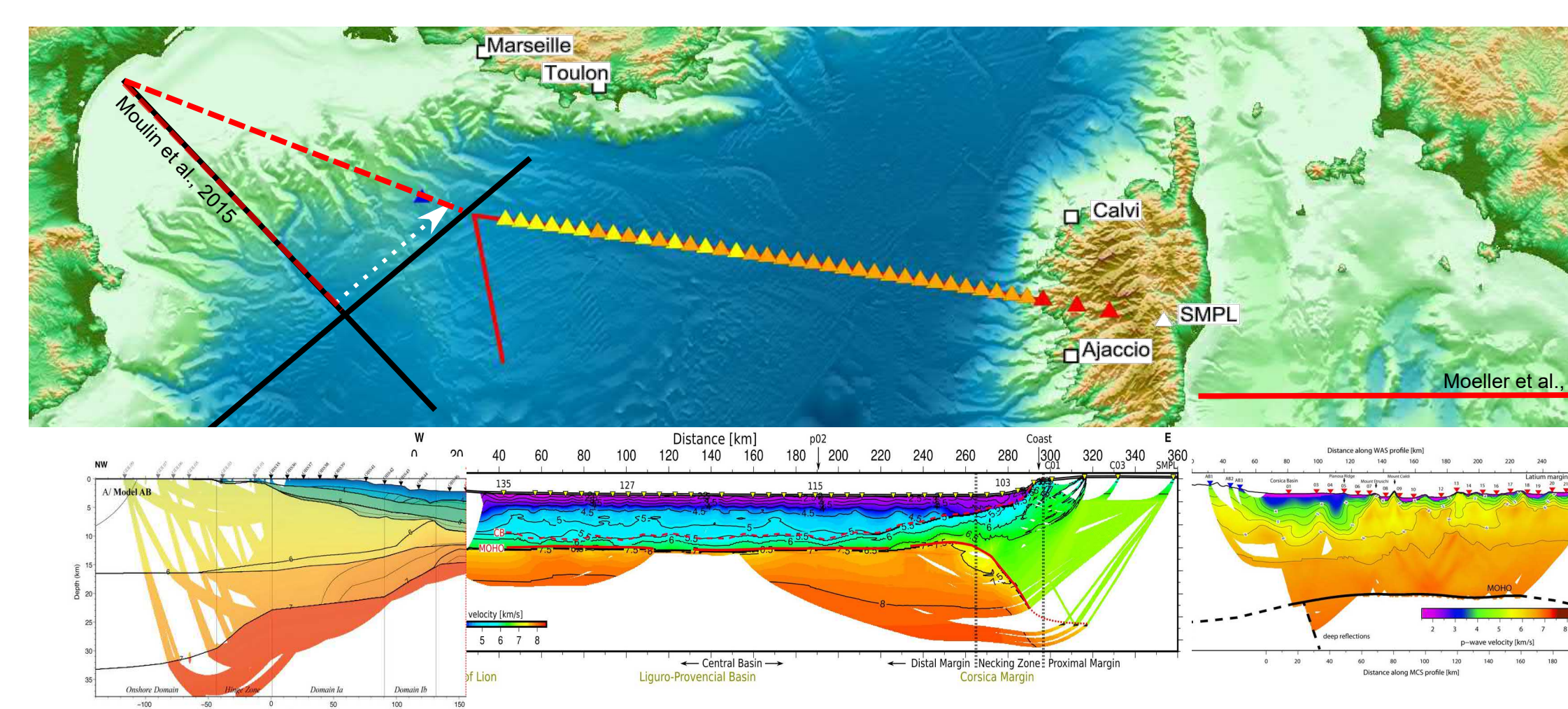


Figure 8: We span a transect from Rom to Perpignan by including previous studies in the Gulf of Lion (projected and stretched from Moulin et al., 2015) and in the Tyrrhenian Sea (Moeller et al., 2013). Different width of the necking zones, however not conjugated parts of the margins.

Failed rifting, mantle exhumation and the necking zone

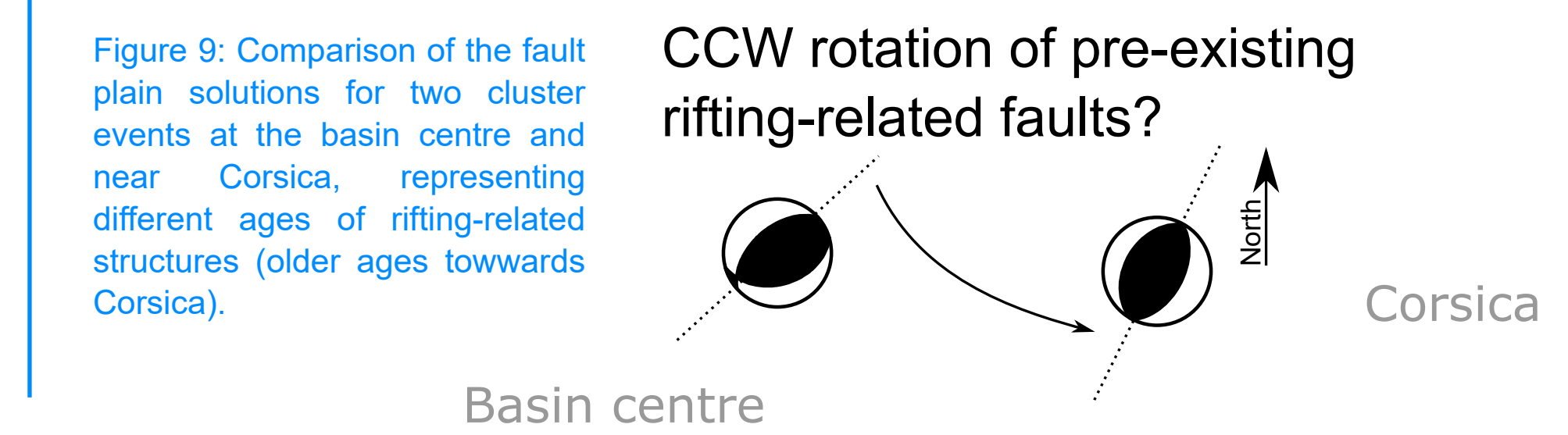
Continental crust is observed along both profiles. Moreover, the earthquakes in the crust and upper mantle indicate brittle, high-angle normal faulting about 80 km west of the necking zone. Delamination at the end of rifting by low-angle detachment faulting leading to exhumation of sub-continental mantle is not observed between 180 km and the necking zone at 280 km along the profile.

- Rifting failed before an oceanic domain was fully developed.
- The observed low seismic velocities in the mantle in the necking zone (260-280 km) might be caused by crustal underplating.

Basin inversion and rheology

Thrust fault earthquakes in the basin centre (Larroque et al., 2016; Thorwart et al., 2021) indicate basin inversion, leading to the closure of the Ligurian Basin.

- Events of the C1 cluster occur in the uppermost mantle.
- Strengthening of the uppermost mantle during rifting
- Events possibly occur in re-activated normal faults that were created during extension. Focal mechanisms between the clusters deviate by ~15° in the strike.
- The events might map the history of the CCW rotation of the Corsica-Sardinia Block (~23°) between ~20-16 Ma.



Conclusions

- Continental crust is observed basin. The continental crust was extremely thinned within a very narrow zone. Based on the seismic and gravity results we conclude that the Oligocene-Miocene extension led to:
- Hyper-extended continental crust across the Ligurian Basin.
 - Extension led to strengthening of the uppermost mantle in the basin.
 - Rifting failed before the formation of oceanic crust.
 - The Ligurian Sea is closing, compressional seismic events occur in rifting-related re-activated faults.

Acknowledgments

This project was funded by Deutsche Forschungsgemeinschaft (DFG), grant number KO_2961/6-1. We thank the captain and crew of RV Maria S. Merian cruise MSM71 for their support. The LOBSTER project comprises the offshore component of the AlpArray seismic network (Hetényi et al., 2018) and is part of the German priority program SPP2017 4D-MB.



References

Carlson and Miller (2003), <https://doi.org/10.1029/2002GL016600>
 Christensen and Mooney (1995), <https://doi.org/10.1029/95JB00259>
 Dannowski et al. (2020), <https://doi.org/10.5194/se-11-873-3030>
 Gueguen et al. (1998), [https://doi.org/10.1016/S0040-1951\(98\)00189-9](https://doi.org/10.1016/S0040-1951(98)00189-9)
 Hetényi et al. (2018), <https://doi.org/10.1007/s10712-018-9472-4>
 Larroque et al. (2016), <https://doi.org/10.1016/j.tecto.2016.03.027>
 Moeller et al. (2013), <https://doi.org/10.1002/jgge.20180>
 Moulin et al. (2015), <https://doi.org/10.2113/gssgblib.186.4-5.309>
 Rollet et al. (2002), <https://doi.org/10.1029/2001TC900027>
 Thorwart et al. (2021), <https://doi.org/10.5194/se-12-2553-2021>